



CERN-EP-2022-066

24 March 2022

Measurement of the J/ψ polarization with respect to the event plane in Pb–Pb collisions at the LHC

ALICE Collaboration

Abstract

The polarization of inclusive J/ψ produced in Pb–Pb collisions at $\sqrt{s_{NN}} = 5.02$ TeV at the LHC was studied by ALICE in the dimuon channel, via the measurement of the angular distribution of its decay products. The study was performed in the rapidity region $2.5 < y < 4$, for three transverse momentum intervals ($2 < p_T < 4$, $4 < p_T < 6$, $6 < p_T < 10$ GeV/ c) and as a function of the centrality of the collision for $2 < p_T < 6$ GeV/ c . For the first time, the polarization was measured with respect to the event plane of the collision, by considering the angle between the positive-charge decay muon in the J/ψ rest frame and the axis perpendicular to the event-plane vector in the laboratory system. A small transverse polarization is measured, with a significance reaching 3.9σ at low p_T and for intermediate centrality values. The polarization could be connected with the existence of a strong magnetic field in the early stage of quark–gluon plasma formation in Pb–Pb collisions, as well as with its behaviour as a rotating fluid with large vorticity.

arXiv:2204.10171v1 [nucl-ex] 21 Apr 2022

Quarkonia, bound states of a heavy quark–antiquark pair, have been studied since a long time because they give access to several features of the strong interaction that can be investigated with various complementary approaches (see Refs. [1, 2] for comprehensive reviews). Calculations based on the Quantum Chromodynamics (QCD) theory formulated on a discrete lattice [3] and non-relativistic potential models [4] can reproduce the rich spectroscopy of the various states corresponding to different radial and angular excitations of the quarkonium wave function. Their production can be described as a two-step process: the heavy-quark pair production, which occurs on short timescales due to the hard scale connected with the mass of the quarks and can be calculated by perturbative QCD, and the binding of the pair, a soft process that has to be described by a non-perturbative treatment. The Non-Relativistic QCD (NRQCD) approach [5] represents the most advanced tool for our understanding of quarkonium production in proton–proton collisions and is able to reproduce the measured cross sections for most states. The produced quarkonia may also exhibit polarization, defined as the alignment of the particle spin with respect to a chosen axis [6]. The polarization can also be calculated in the framework of NRQCD, and although for some states discrepancies between theory and experiment persist until today, a reasonable understanding of quarkonium production and polarization has been reached [7–9]. Other approaches, such as the Improved Color Evaporation Model (ICEM) [10], are shown to reproduce quarkonium measurements at collider energies fairly well.

Quarkonium states may also be used as a probe of the environment in which they are created or they traverse during their evolution. Their binding energy and more generally their spectral functions may be altered [11, 12] due to the presence of a quark–gluon plasma (QGP), a high energy-density state of strongly interacting matter formed in ultrarelativistic heavy-ion collisions and currently studied at RHIC and the LHC (at center-of-mass energies per nucleon–nucleon collision, $\sqrt{s_{NN}}$, up to 0.2 and 5.02 TeV, respectively). These hot matter effects may lead to the dissociation or prevent the formation of the bound $q\bar{q}$ state. Studies in this direction have been carried out for decades and the experimental measurements [13–15] can be understood in terms of sequential dissociation affecting charmonium ($c\bar{c}$) and bottomonium ($b\bar{b}$) according to the binding energy of the various spectroscopic states and as a function of the temperature of the QGP [16, 17]. Furthermore, charmonia can also be significantly regenerated in the QGP phase and/or when the QGP hadronizes [18–20], in particular when the initial multiplicity of produced charm quarks is large (e.g., $> 10^2$ for central Pb–Pb collisions at the LHC).

In addition to the quarkonium yield modifications in ultrarelativistic heavy-ion collisions, one might expect the polarization of surviving quarkonia to be altered because of other specific features of the environment. Such collisions are indeed known to produce the strongest electromagnetic fields that can be produced in the laboratory, and possibly in nature [21, 22]. In particular, the fast motion of the charges of the nuclei can produce a magnetic field oriented perpendicular to the reaction plane, defined by the vector of the impact parameter of the collision and the beam direction, and possibly exceeding 10^{20} Gauss at LHC energies [22, 23]. The maximum value of the field generated by this mechanism increases with energy (by a factor ~ 10 between RHIC and the LHC), is reached very shortly ($\ll 1$ fm/c) after collision time [21], and is expected to decrease by several orders of magnitude by $t = 1$ fm/c [24]. However, due to the formation of a QGP and to its finite electrical conductivity, large magnetic field values may be sustained along its entire lifetime. The production of a heavy quark pair also happens early in the collision history, within typical timescales of the order of $t \sim 1/(2m_q) \sim 0.1$ fm/c [25], and with the subsequent evolution towards a bound state also occurring on a time range < 1 fm/c [26, 27], implying that polarization of charmonia may be influenced by the presence of the strong magnetic field generated in the collisions.

Another effect that may alter the polarization of quarkonia, via spin-orbit coupling, is the generation of a huge orbital angular momentum of the medium, again directed along the perpendicular to the reaction plane [28, 29]. In the hydrodynamic description of the QGP, this amounts to the creation of a rotating fluid with a large vorticity, with estimated values up to $\sim 10^{22}$ s⁻¹ [30], much larger than any other

fluid existing in the universe. Among the related effects, the polarization of Λ hyperons [30, 31] was discovered by STAR, and a spin alignment of the ϕ and K^{*0} vector mesons (spin quantum number equal to unity) [32, 33] was observed by the ALICE experiment. These hadrons are expected to be formed, up to a few GeV/c transverse momentum, by light and strange quarks produced in the QGP, via recombination processes occurring close in time to the hadronization transition. The charmonium vector mesons produced by regeneration effects, in particular at low p_T , may therefore also exhibit spin alignment effects as it is the case for light vector mesons. These effects can be parameterized in terms of the ρ_{00} element of the spin-density matrix [34] or, as is most customary in the study of quarkonium polarization, via the λ_θ parameter in the expression giving the polar angle distribution $W(\theta)$ of the dilepton decay products of charmonium vector states [6]:

$$W(\theta) \propto \frac{1}{3 + \lambda_\theta} (1 + \lambda_\theta \cos^2 \theta), \quad (1)$$

where θ is the polar angle emission of the positively charged decay lepton, with respect to a chosen axis. It can be shown that $\lambda_\theta \propto (3\rho_{00} - 1)/(1 - \rho_{00})$, so that the finite spin-alignment condition $\rho_{00} \neq 1/3$ is equivalent to the finite polarization condition $\lambda_\theta \neq 0$.

In this Letter, we report the first measurement of the J/ψ polarization with respect to an axis perpendicular to the event plane, carried out by ALICE in Pb–Pb collisions at $\sqrt{s_{NN}} = 5.02$ TeV. The results refer to inclusive J/ψ, i.e., both prompt (direct production and contribution from decays of higher-mass charmonium states) and non-prompt (from decays of hadrons containing a b quark), with the latter accounting for less than 15% in the covered p_T range [35]. The only previously published result on J/ψ polarization for this collision system was also obtained by ALICE [36], by measuring, via the decay $J/\psi \rightarrow \mu^+ \mu^-$, the J/ψ polarization in the helicity and Collins–Soper reference frames. These measurements showed deviations from $\lambda_\theta = 0$ with a $\sim 2.1\sigma$ maximum significance at low p_T , for both reference frames. In these two reference frames the polarization was measured with respect to directions directly connected with the production process, i.e., the momentum direction of the J/ψ itself (helicity) or the direction of motion of the colliding hadrons (Collins–Soper). By measuring the polarization with respect to the estimated reaction plane of the nuclear collision, as done in this analysis, one rather selects a reference frame that should naturally be connected with the observation of polarization effects due to the presence of early electromagnetic fields and/or QGP vorticity.

The data analyzed in this Letter were collected by ALICE in 2015 and 2018, and the J/ψ decay to muon pairs was studied in the muon spectrometer, which covers the pseudorapidity region $-4 < \eta < -2.5$. This detector, as well as the complete ALICE set-up, is described in detail in Refs. [37, 38]. Briefly, the muon spectrometer consists of a 3 T-m dipole magnet and a system of five tracking (Cathode Pad Chambers) and two triggering stations (Resistive Plate Chambers). Two hadron absorbers, respectively 10 and 7.2 interaction lengths thick, separate the interaction region from the tracking system, and the tracking and triggering systems. The other detectors used for this analysis are: (i) the two layers of the Silicon Pixel Detector, SPD ($|\eta| < 2$ and $|\eta| < 1.4$), which represent the innermost part of the ALICE central barrel and are used for the determination of the position of the primary interaction vertex and the estimate of the event plane of the collision; (ii) the two V0 scintillator arrays ($-3.7 < \eta < -1.7$ and $2.8 < \eta < 5.1$), which provide the minimum bias (MB) trigger, given by a coincidence of signals from their two sides, and are used for the rejection of beam–gas interactions. They are also used for the determination of the centrality of the collisions (see below) and for the estimate of the resolution of the event-plane determination; (iii) the Zero Degree Calorimeters located on either side of the interaction point at 112.5 m along the beam axis, which detect spectator nucleons emitted at zero degrees with respect to the LHC beam axis and are used to reject electromagnetic Pb–Pb interactions.

The analysed events were recorded using a dimuon trigger, defined as the coincidence of a MB trigger together with the detection of two opposite-sign candidate tracks in the triggering system of the muon

spectrometer. The trigger algorithm applies a non-sharp p_T cut, which has 50% efficiency at 1 GeV/c and becomes fully efficient (> 98%) beyond $p_T \sim 2$ GeV/c. Selection criteria were applied at the single muon and muon pair level (see Refs. [20, 36, 39] for details). In particular, tracks reconstructed in the tracking system were required to point at the interaction vertex and should match a corresponding track in the trigger system. The radial position of the tracks at the end of the front absorber must be in the range $17.6 < R < 89.5$ cm and their pseudorapidity range within $-4 < \eta_\mu < -2.5$. Opposite-sign dimuons were selected in the rapidity interval $2.5 < y < 4$ ¹ and invariant mass range $2.1 < m_{\mu\mu} < 4.9$ GeV/c².

The events were classified from central to peripheral according to the decreasing energy deposition in the V0 system, which is directly connected to the degree of geometric overlap of the colliding nuclei [40]. For the analysis the most central 90% of the hadronic cross section was selected, which ensures full efficiency of the MB selection, with negligible contamination from electromagnetic processes.

The event-plane angle was estimated, event per event, as the 2nd harmonic symmetry plane of charged particles at midrapidity, $\Psi_2 = \tan^{-1}(Q_{2,y}/Q_{2,x})/2$, where the transverse components of the flow vector Q_2 were obtained as $Q_{2,x} = \sum_i \cos(2\varphi_i)$ and $Q_{2,y} = \sum_i \sin(2\varphi_i)$, with φ_i being the azimuthal angle of the i^{th} tracklet defined by combinations of hits in the SPD. A recentering procedure [41] was performed, as a function of the longitudinal position of the primary vertex, to remove non-uniformities in the SPD acceptance.

Each dimuon was weighted by the inverse of the product of its acceptance times reconstruction efficiency ($A \times \varepsilon$), assuming it comes from the decay of a J/ψ. A Monte Carlo simulation was used for the calculation of $A \times \varepsilon$, with the generated J/ψ signal being injected inside real MB events, to properly reproduce the effect of detector occupancy and its variation from one centrality class to another. The y and p_T input distributions for the J/ψ were taken from Ref. [20], while a flat distribution was assumed for the cosine of the polar angle (θ) distribution with respect to the event plane. A significant p_T dependence of the shape of $A \times \varepsilon$ as a function of $\cos \theta$ was found, and for this reason the correction was performed on a fine 2D grid in $\cos \theta$ vs p_T . Thanks to a narrow binning that leads to a small variation of these variables in each cell, the corresponding $A \times \varepsilon$ values were found to be only minorly sensitive to variations in the input distributions. It was also checked that the small correlations between rapidity and transverse momentum distributions of the J/ψ, which were measured by LHCb in pp collisions at $\sqrt{s} = 7$ TeV [35], do not induce any significant modification in the angular acceptance. The calculations were also performed as a function of the collision centrality. While the values of $A \times \varepsilon$ decrease by $\sim 15\%$ from peripheral to central events, the shape of their angular distributions does not change appreciably. Typical values of $A \times \varepsilon$ are $\sim 10\%$ around $\cos \theta = 0$ and increase by a factor 2–2.5 when $|\cos \theta| = 1$.

The extraction of the polarization parameter λ_θ was carried out as a function of centrality, for the transverse momentum interval $2 < p_T < 6$ GeV/c, and as a function of p_T for the centrality intervals 0–20% and 30–50%. For each range in centrality and p_T the $A \times \varepsilon$ -corrected invariant mass distributions were separately obtained for 10 $\cos \theta$ intervals in $-1 < \cos \theta < 1$. The number of J/ψ for each interval was obtained by means of a χ^2 minimization fit, with the signal being described by a double-sided Crystal Ball function or a pseudo-Gaussian with a mass-dependent width [42]. The central value of the mass and the width of the J/ψ were kept as free parameters of the fit, while the non-Gaussian tail parameters were fixed to the Monte Carlo values. The small contribution from the $\psi(2S)$ was included, but was found to have a negligible influence on the fit result. The background was empirically reproduced by a fourth-degree polynomial times an exponential, or a pseudo-Gaussian with a width quadratically dependent on the mass. The fits have χ^2/ndf values ranging from 0.6 to 1.8. The minimum value of the signal over background ratio is 0.12 and the corresponding significance of the signal is 36, with an increase from central to peripheral collisions and from low to high p_T . Finally, the λ_θ values were obtained by fitting the $\cos \theta$ distributions of the positive-sign decay muons from the J/ψ according to Eq. 1. In Fig. 1, an

¹Due to the symmetry of the collision system, a positive notation was adopted.

example of a fit to $A \times \varepsilon$ -corrected angular distributions is shown, corresponding to the centrality range 30–50% and $2 < p_T < 4$ GeV/c. Also shown in Fig. 1 is the result of a similar analysis where for each event the event-plane angle was replaced by a randomly chosen direction. A flat angular distribution for the J/ψ was obtained in the latter case. For all the fits corresponding to the various combinations of transverse momentum and centrality intervals, the values of λ_θ extracted with a random assignment of the event plane were compatible with zero, within at most 1σ . Finally, λ_θ must be corrected for the finite resolution on the event-plane determination. The procedure follows the one used for the K^{*0} and ϕ mesons spin alignment measurement [32] which was proposed in Ref. [43], where a simple relation between the true and observed values of the spin-density matrix element, involving the event plane resolution, was given. The centrality-dependent resolution was estimated, in narrow intervals, for the analysis of the J/ψ elliptic flow [44], with maximum values around 0.8–0.9, decreasing for very central and peripheral events. Then, average values weighted with the number of reconstructed J/ψ in each narrow centrality interval were computed in order to obtain the event plane resolution for the relatively wide centrality ranges studied in this analysis. The extracted correction factors have a modest impact on the values of λ_θ , the largest variation being +0.02.

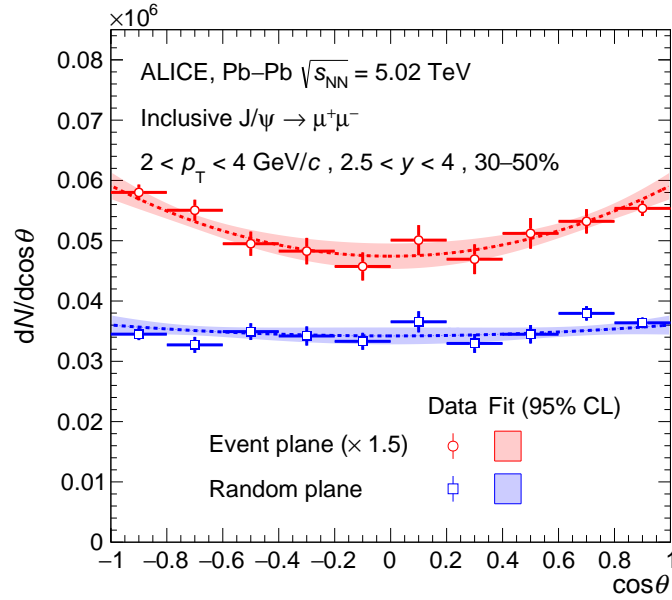


Figure 1: Fit to the $(A \times \varepsilon)$ -corrected angular distribution of the positive muons from the J/ψ decay, for the interval $2 < p_T < 4$ GeV/c and the centrality range 30–50% (red points and curve). Only statistical uncertainties are shown for the data points. The shaded area represents the uncertainty associated with the fit. Also shown (blue points and curve) is the result of a control analysis where, for each event, the estimated event plane was rotated by a random angle.

The systematic uncertainties on the evaluation of λ_θ are related to the extraction of the J/ψ signal, to the kinematic distributions used as inputs to the Monte Carlo simulation and to the estimate of the dimuon trigger efficiency. The first source of uncertainty was evaluated by comparing the λ_θ values obtained from angular distributions extracted with different choices for the signal and background shapes in the invariant mass fits, and by using various fit ranges, from $2.1 < m_{\mu\mu} < 4.9$ GeV/c² (wider) to $2.5 < m_{\mu\mu} < 4.5$ GeV/c² (narrower). The absolute values of this systematic uncertainty, taken as the RMS of the λ_θ values, range between 0.02 and 0.04 as a function of centrality and from 0.02 to 0.06 as a function of p_T . Concerning the Monte Carlo generation, due to suppression and regeneration effects on the J/ψ yields occurring in Pb–Pb collisions [20], the p_T and y distributions have a centrality dependence. A weight to the default centrality-integrated distributions was applied in order to reproduce such dependence in

the $A \times \varepsilon$ calculations. The effect on the evaluation of λ_θ was found to be small, being less than 0.01 as a function of centrality, and smaller than 0.02 as a function of transverse momentum. Finally, the systematic uncertainty associated to the trigger efficiency was evaluated. Since the muon trigger response function exhibits a slight difference in data and in the Monte Carlo for $p_T < 2$ GeV/c, the λ_θ parameter was extracted after weighting the $A \times \varepsilon$ in order to take into account this discrepancy. The variation of the results after this correction was taken as the systematic uncertainty which stays constant at ~ 0.01 as a function of centrality, and varies between 0.01 and 0.02 as a function of the transverse momentum. In ALICE data analyses involving muon detection, further efficiency-related uncertainties are usually assigned (tracking, matching between tracks/tracklets in the tracking/trigger detectors) by comparing the evaluation of these efficiencies from Monte Carlo and from data. It was checked that the ratio between the angular distributions obtained considering such different evaluations is constant. As a consequence, the results on the polarization parameter are not affected. The total systematic uncertainty on λ_θ was obtained as the quadratic sum of the values corresponding to each source, with numerical values being reported in Table 1.

Table 1: Systematic uncertainties on the evaluation of the λ_θ parameter. The quoted uncertainties for the various sources are considered as uncorrelated.

p_T (GeV/c)	Centrality	Signal	Trigger	Input MC	Total
2–6	0–20%	0.045	0.006	0.006	0.046
	20–40%	0.027	0.010	0.006	0.030
	40–60%	0.015	0.006	0.002	0.017
	60–90%	0.016	0.007	0.003	0.018
Centrality	p_T (GeV/c)	Signal	Trigger	Input MC	Total
0–20%	2–4	0.063	0.017	0.007	0.065
	4–6	0.020	0.011	0.007	0.024
	6–10	0.024	0.006	0.008	0.026
30–50%	2–4	0.032	0.007	0.006	0.033
	4–6	0.026	0.015	0.008	0.031
	6–10	0.025	0.006	0.012	0.029

In Fig. 2, the centrality dependence of λ_θ for the transverse momentum range $2 < p_T < 6$ GeV/c is presented (left panel), as well as the transverse momentum dependence of λ_θ for central (0–20%) and intermediate centrality (30–50%) events (right panel). As a function of centrality a small but significant non-zero polarization is found from central collisions down to the 40–60% centrality interval, where a 3.5σ effect is observed. The results as a function of p_T may indicate that the deviation from zero is larger at small transverse momentum. The maximum deviation from $\lambda_\theta = 0$ as a function of transverse momentum is observed for $2 < p_T < 4$ GeV/c and 30–50% centrality where, considering the total uncertainty, a 3.9σ effect is present. The results correspond to inclusive J/ψ production, implying that a small contribution from a potential polarization of parent beauty hadrons, which could anyway be diluted in the decay process [45], might be present.

Previous measurements carried out by ALICE on K^{*0} and ϕ spin alignment [32] had established evidence of a significant effect for vector mesons in heavy-ion collisions, stronger at low p_T and for semi-central Pb–Pb collisions. However, the maximum λ_θ value measured for the J/ψ (~ 0.2) in this analysis would translate, in the language of spin matrix elements, to $\rho_{00} \sim 0.37$. This result implies a positive deviation of +0.04 from $\rho_{00} = 1/3$ (corresponding to no spin alignment), in the opposite direction and by a smaller absolute amount with respect to the corresponding deviations of about -0.2 for K^{*0} and -0.1 for ϕ . It must anyway be stressed that, in spite of the similar quantum numbers, the J/ψ production process in nuclear collisions at the LHC is different from that of mesons containing light and strange quarks. In fact, while K^{*0} and ϕ are mainly expected to be produced by quark recombination processes at QGP hadronization

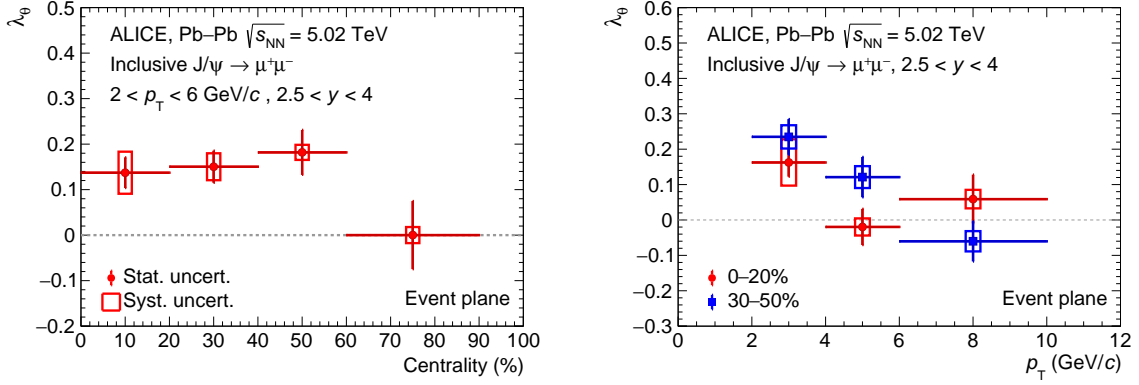


Figure 2: Centrality (left panel) and p_T dependence (right panel) of λ_θ . The vertical bars represent the statistical uncertainties, while the boxes correspond to the systematic uncertainties. The horizontal bars show the size of the corresponding centrality and p_T ranges, with the data points being located at the center of each interval.

and even later in the hadronic phase [46], J/ψ production can occur both in the QGP phase, thanks to the early production of charm quarks in hard processes, and at hadronization, via recombination of charm quarks, with the latter mechanism becoming dominant at low p_T [47]. The spin alignment observed in this analysis for the J/ψ , which is larger at low p_T , may point to an origin in common to that generating this effect for K^{*0} and ϕ in the same kinematic region. On the other hand the tendency for such alignment to vanish at higher p_T may indicate that effects active in the early stages of the collision (strong magnetic fields) may be less effective in generating a net polarization for charmonia. Clearly, these hints need to be confirmed by theory studies devoted to charm and charmonium production, that are not available as of today.

In summary, we have reported on the first measurement of the polarization for inclusive J/ψ produced in Pb–Pb interactions at $\sqrt{s_{NN}} = 5.02$ TeV, carried out by ALICE using the direction perpendicular to the event plane of the collision as the polarization axis. This choice makes this measurement potentially sensitive to the strong magnetic field created in high-energy nuclear collisions, as well as to vorticity effects in the QGP state. A small but significant polarization effect, reaching 3.9σ for $2 < p_T < 4$ GeV/c and 30–50% centrality, is measured. In absolute terms, the effect is smaller than that seen for light vector mesons. However, significant differences in the production processes require dedicated theory studies for a quantitative understanding of this observation and a precise connection with the QGP properties at its origin.

References

- [1] N. Brambilla *et al.*, “Heavy quarkonium: progress, puzzles, and opportunities”, *Eur. Phys. J. C* **71** (2011) 1534, arXiv:1010.5827 [hep-ph].
- [2] A. Andronic *et al.*, “Heavy-flavour and quarkonium production in the LHC era: from proton-proton to heavy-ion collisions”, *Eur. Phys. J. C* **76** no. 3, (2016) 107, arXiv:1506.03981 [nucl-ex].
- [3] **HPQCD, UKQCD, MILC, Fermilab Lattice** Collaboration, C. T. H. Davies *et al.*, “High precision lattice QCD confronts experiment”, *Phys. Rev. Lett.* **92** (2004) 022001, arXiv:hep-lat/0304004.
- [4] E. Eichten, K. Gottfried, T. Kinoshita, K. D. Lane, and T.-M. Yan, “Charmonium: The Model”, *Phys. Rev. D* **17** (1978) 3090. [Erratum: *Phys.Rev.D* 21, 313 (1980)].

- [5] G. T. Bodwin, E. Braaten, and G. P. Lepage, “Rigorous QCD analysis of inclusive annihilation and production of heavy quarkonium”, *Phys. Rev.* **D51** (1995) 1125–1171, arXiv:hep-ph/9407339 [hep-ph]. [Erratum: *Phys. Rev.*D55,5853(1997)].
- [6] P. Faccioli, C. Lourenco, J. Seixas, and H. K. Wohri, “Towards the experimental clarification of quarkonium polarization”, *Eur. Phys. J.* **C69** (2010) 657–673, arXiv:1006.2738 [hep-ph].
- [7] G. T. Bodwin, K.-T. Chao, H. S. Chung, U.-R. Kim, J. Lee, and Y.-Q. Ma, “Fragmentation contributions to hadroproduction of prompt J/ψ , χ_{cJ} , and $\psi(2S)$ states”, *Phys. Rev. D* **93** no. 3, (2016) 034041, arXiv:1509.07904 [hep-ph].
- [8] Y.-Q. Ma, T. Stebel, and R. Venugopalan, “ J/ψ polarization in the CGC+NRQCD approach”, *JHEP* **12** (2018) 057, arXiv:1809.03573 [hep-ph].
- [9] Y. Feng, B. Gong, C.-H. Chang, and J.-X. Wang, “Remaining parts of the long-standing J/ψ polarization puzzle”, *Phys. Rev.* **D99** no. 1, (2019) 014044, arXiv:1810.08989 [hep-ph].
- [10] Y.-Q. Ma and R. Vogt, “Quarkonium Production in an Improved Color Evaporation Model”, *Phys. Rev. D* **94** no. 11, (2016) 114029, arXiv:1609.06042 [hep-ph].
- [11] T. Matsui and H. Satz, “ J/ψ Suppression by Quark-Gluon Plasma Formation”, *Phys. Lett.* **B178** (1986) 416–422.
- [12] A. Rothkopf, “Heavy Quarkonium in Extreme Conditions”, *Phys. Rept.* **858** (2020) 1–117, arXiv:1912.02253 [hep-ph].
- [13] NA50 Collaboration, B. Alessandro *et al.*, “ ψ' production in Pb-Pb collisions at 158-GeV/nucleon”, *Eur. Phys. J. C* **49** (2007) 559–567, arXiv:nuc1-ex/0612013.
- [14] CMS Collaboration, A. M. Sirunyan *et al.*, “Measurement of prompt and nonprompt charmonium suppression in PbPb collisions at 5.02 TeV”, *Eur. Phys. J. C* **78** no. 6, (2018) 509, arXiv:1712.08959 [nucl-ex].
- [15] CMS Collaboration, A. M. Sirunyan *et al.*, “Measurement of nuclear modification factors of $Y(1S)$, $Y(2S)$, and $Y(3S)$ mesons in PbPb collisions at $\sqrt{s_{NN}} = 5.02$ TeV”, *Phys. Lett. B* **790** (2019) 270–293, arXiv:1805.09215 [hep-ex].
- [16] S. Digal, P. Petreczky, and H. Satz, “Quarkonium feed down and sequential suppression”, *Phys. Rev.* **D64** (2001) 094015, arXiv:hep-ph/0106017 [hep-ph].
- [17] B. Krouppa, A. Rothkopf, and M. Strickland, “Bottomonium suppression using a lattice QCD vetted potential”, *Phys. Rev.* **D97** no. 1, (2018) 016017, arXiv:1710.02319 [hep-ph].
- [18] P. Braun-Munzinger and J. Stachel, “(Non)thermal aspects of charmonium production and a new look at J/ψ suppression”, *Phys. Lett.* **B490** (2000) 196–202, arXiv:nuc1-th/0007059 [nucl-th].
- [19] R. L. Thews, M. Schroedter, and J. Rafelski, “Enhanced J/ψ production in deconfined quark matter”, *Phys. Rev.* **C63** (2001) 054905, arXiv:hep-ph/0007323 [hep-ph].
- [20] ALICE Collaboration, S. Acharya *et al.*, “Studies of J/ψ production at forward rapidity in Pb-Pb collisions at $\sqrt{s_{NN}} = 5.02$ TeV”, *JHEP* **02** (2020) 041, arXiv:1909.03158 [nucl-ex].
- [21] V. Skokov, A. Y. Illarionov, and V. Toneev, “Estimate of the magnetic field strength in heavy-ion collisions”, *Int. J. Mod. Phys. A* **24** (2009) 5925–5932, arXiv:0907.1396 [nucl-th].

- [22] W.-T. Deng and X.-G. Huang, “Event-by-event generation of electromagnetic fields in heavy-ion collisions”, *Phys. Rev. C* **85** (2012) 044907, arXiv:1201.5108 [nucl-th].
- [23] P. Christakoglou, S. Qiu, and J. Staa, “Systematic study of the chiral magnetic effect with the AVFD model at LHC energies”, *Eur. Phys. J. C* **81** no. 8, (2021) 717, arXiv:2106.03537 [nucl-th].
- [24] D. E. Kharzeev, L. D. McLerran, and H. J. Warringa, “The Effects of topological charge change in heavy ion collisions: ‘Event by event P and CP violation’”, *Nucl. Phys. A* **803** (2008) 227–253, arXiv:0711.0950 [hep-ph].
- [25] S. K. Das, S. Plumari, S. Chatterjee, J. Alam, F. Scardina, and V. Greco, “Directed Flow of Charm Quarks as a Witness of the Initial Strong Magnetic Field in Ultra-Relativistic Heavy Ion Collisions”, *Phys. Lett. B* **768** (2017) 260–264, arXiv:1608.02231 [nucl-th].
- [26] J. Hufner, Y. P. Ivanov, B. Z. Kopeliovich, and A. V. Tarasov, “Photoproduction of charmonia and total charmonium proton cross-sections”, *Phys. Rev. D* **62** (2000) 094022, arXiv:hep-ph/0007111.
- [27] D. Kharzeev and R. L. Thews, “Quarkonium formation time in a model independent approach”, *Phys. Rev. C* **60** (1999) 041901, arXiv:nucl-th/9907021.
- [28] Z.-T. Liang and X.-N. Wang, “Globally polarized quark-gluon plasma in non-central A+A collisions”, *Phys. Rev. Lett.* **94** (2005) 102301, arXiv:nucl-th/0410079. [Erratum: *Phys.Rev.Lett.* 96, 039901 (2006)].
- [29] F. Becattini, F. Piccinini, and J. Rizzo, “Angular momentum conservation in heavy ion collisions at very high energy”, *Phys. Rev. C* **77** (2008) 024906, arXiv:0711.1253 [nucl-th].
- [30] **STAR** Collaboration, L. Adamczyk *et al.*, “Global Λ hyperon polarization in nuclear collisions: evidence for the most vortical fluid”, *Nature* **548** (2017) 62–65, arXiv:1701.06657 [nucl-ex].
- [31] **ALICE** Collaboration, S. Acharya *et al.*, “Global polarization of Λ and $\bar{\Lambda}$ hyperons in Pb-Pb collisions at $\sqrt{s_{NN}} = 2.76$ and 5.02 TeV”, *Phys. Rev. C* **101** no. 4, (2020) 044611, arXiv:1909.01281 [nucl-ex].
- [32] **ALICE** Collaboration, S. Acharya *et al.*, “Evidence of Spin-Orbital Angular Momentum Interactions in Relativistic Heavy-Ion Collisions”, *Phys. Rev. Lett.* **125** no. 1, (2020) 012301, arXiv:1910.14408 [nucl-ex].
- [33] **STAR** Collaboration, B. I. Abelev *et al.*, “Spin alignment measurements of the $K^{*0}(892)$ and $\phi(1020)$ vector mesons in heavy ion collisions at $\sqrt{s_{NN}} = 200$ GeV”, *Phys. Rev. C* **77** (2008) 061902, arXiv:0801.1729 [nucl-ex].
- [34] K. Schilling, P. Seyboth, and G. E. Wolf, “On the Analysis of Vector Meson Production by Polarized Photons”, *Nucl. Phys. B* **15** (1970) 397–412. [Erratum: *Nucl.Phys.B* 18, 332 (1970)].
- [35] **LHCb** Collaboration, R. Aaij *et al.*, “Measurement of J/ψ production in pp collisions at $\sqrt{s} = 7$ TeV”, *Eur. Phys. J. C* **71** (2011) 1645, arXiv:1103.0423 [hep-ex].
- [36] **ALICE** Collaboration, S. Acharya *et al.*, “First measurement of quarkonium polarization in nuclear collisions at the LHC”, *Phys. Lett. B* **815** (2021) 136146, arXiv:2005.11128 [nucl-ex].
- [37] **ALICE** Collaboration, K. Aamodt *et al.*, “The ALICE experiment at the CERN LHC”, *JINST* **3** (2008) S08002.

- [38] **ALICE** Collaboration, B. Abelev *et al.*, “Performance of the ALICE Experiment at the CERN LHC”, *Int. J. Mod. Phys. A* **29** (2014) 1430044, arXiv:1402.4476 [nucl-ex].
- [39] **ALICE** Collaboration, S. Acharya *et al.*, “Study of J/ψ azimuthal anisotropy at forward rapidity in Pb-Pb collisions at $\sqrt{s_{NN}} = 5.02$ TeV”, *JHEP* **02** (2019) 012, arXiv:1811.12727 [nucl-ex].
- [40] **ALICE** Collaboration, B. Abelev *et al.*, “Centrality determination of Pb-Pb collisions at $\sqrt{s_{NN}} = 2.76$ TeV with ALICE”, *Phys. Rev. C* **88** no. 4, (2013) 044909, arXiv:1301.4361 [nucl-ex].
- [41] I. Selyuzhenkov and S. Voloshin, “Effects of non-uniform acceptance in anisotropic flow measurement”, *Phys. Rev. C* **77** (2008) 034904, arXiv:0707.4672 [nucl-th].
- [42] **ALICE** Collaboration, J. Adam *et al.*, “Quarkonium signal extraction in ALICE”, ALICE-PUBLIC-2015-006. <https://cds.cern.ch/record/2060096>.
- [43] A. H. Tang, B. Tu, and C. S. Zhou, “Practical considerations for measuring global spin alignment of vector mesons in relativistic heavy ion collisions”, *Phys. Rev. C* **98** no. 4, (2018) 044907, arXiv:1803.05777 [nucl-ex].
- [44] **ALICE** Collaboration, S. Acharya *et al.*, “J/ψ elliptic and triangular flow in Pb-Pb collisions at $\sqrt{s_{NN}} = 5.02$ TeV”, *JHEP* **10** (2020) 141, arXiv:2005.14518 [nucl-ex].
- [45] **CDF** Collaboration, A. Abulencia *et al.*, “Polarization of J/ψ and ψ(2S) Mesons Produced in p̄p Collisions at $\sqrt{s} = 1.96$ -TeV”, *Phys. Rev. Lett.* **99** (2007) 132001, arXiv:0704.0638 [hep-ex].
- [46] **ALICE** Collaboration, S. Acharya *et al.*, “Production of K*(892)⁰ and φ(1020) in pp and Pb-Pb collisions at $\sqrt{s_{NN}} = 5.02$ TeV”, arXiv:2106.13113 [nucl-ex].
- [47] **ALICE** Collaboration, B. Abelev *et al.*, “Centrality, rapidity and transverse momentum dependence of J/ψ suppression in Pb-Pb collisions at $\sqrt{s_{NN}}=2.76$ TeV”, *Phys. Lett.* **B734** (2014) 314–327, arXiv:1311.0214 [nucl-ex].